IEEE Access
Multidisciplinary | Rapid Review | Open Access Journal

Received May 18, 2020, accepted May 27, 2020, date of publication June 2, 2020, date of current version June 17, 2020.

Digital Object Identifier 10.1109/ACCESS.2020.2999437

Design and Development of a Movable and Self-Extensible Apparatus for Substation Construction and Maintenance

JUAN WEI[1], DIANSHENG LUO[1], (Member, IEEE), BOZHONG WANG[2], HONGYING HE[1], (Member, IEEE), JINMING LI[3], AND YULIN LUO[2]

[1]College of Electrical and Information Engineering, Hunan University, Changsha 410082, China
[2]State Grid Hunan Electric Power Corporation Maintenance Company, Changsha 410004, China
[3]State Grid Hunan Electric Power Corporation Economic and Technical Research Institute, Changsha 410004, China

Corresponding author: Diansheng Luo (lhx20070322@hnu.edu.cn)

This work was supported in part by the National Natural Science Foundation of China under Grant 51722701, in part by the Natural Science Foundation of Hunan Province, China, 2019, under Grant 2019JJ40019, and in part by the National Key Research and Development Plan, China, 2017, under Grant 2017YFB0903403.

ABSTRACT The increasing requirements of security operation and service quality have brought challenges to the construction and maintenance of the smart substation. In this paper, a movable and self-extensible apparatus is developed for enhancing the security and efficiency of substation construction and electrical infrastructure maintenance. The designed apparatus is equipped with a complete set of pneumatic and electric tools to achieve the integration and fastening of small electrical parts. Moreover, the developed apparatus structure can be self-extensible and self-propelled by automatically controlling the servo-drive system. Considering the extreme weather events such as strong wind, snowstorm, and the integrated blizzard conditions, the overall framework and control system of the apparatus is designed based on the finite element method, and the modal analysis and static analysis are implemented to verify stability and rigidity for the assembled apparatus frame. The security evaluation results and on-site application indicate that the apparatus can effectively enhance the security of maintenance personnel and work efficiency with characteristics of low cost, automatic control, excellent insulation, easy operation as well as high reliability.

INDEX TERMS Electrical infrastructure, maintenance, finite element method, substation construction, prosumer substation.

I. INTRODUCTION

With the increasing penetration of intermittent energy and the rapid development of smart grid technology, the security and efficiency of substation construction and electrical infrastructure maintenance have received widespread attention [1]. The smart substation which serves as a typical energy hub for electric energy transfer, monitoring, control, and secure operation [2], is recently growing dramatically all over the world. According to the statistics from the State Grid Corporation of China, the total substation amount in China has increased from approximately 21500 in 2007 to 41300 in 2018 [3], and the electrical equipment scale is increasing exponentially. The increasing requirements of security operation level and service quality have brought challenges to the construction and operation maintenance of the smart substation.

The growing penetration of distributed energy resources has made it possible for traditional passive consumers to evolve into active prosumers [4]. The prosumer can realize the management of their energy generation, storage, and consumption simultaneously through their electrical infrastructure. For a large-scale wind farm, photovoltaic (PV) and prosumer substations construction, a series of problems [5]–[8] have been raised with the severe influence in the practical work, such as high cost, leakage risk, hidden accidents of personnel and equipment, and so on. Besides, the professional personnel is not enough to accomplish the heavy workload of operation and maintenance of substation infrastructure. Therefore, the auxiliary apparatus development for on-site construction becomes an essential task to

The associate editor coordinating the review of this manuscript and approving it for publication was Huai-zhi Wang.

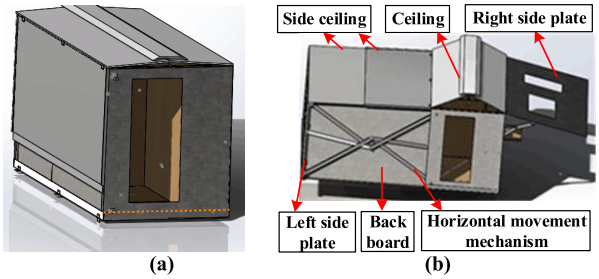

FIGURE 1. Apparatus Frameworks: (a) normality mode, (b) extension mode.

improve work efficiency and ensure the safety of personnel and electrical equipment in practical engineering.

To address these problems, the idea of the container was introduced to deal with goods carriage in the field of on-site construction, ports, mining, and other regions [9]–[11]. The multi-layer modular of the container is easy to assemble on-site but not suitable for people to live or use. The enlarged container with an improved building-based container model was developed to meet the practical requirement for professional personnel [12]. The mechanical performances [13] and universal load conditions [14] of the modular container were analyzed and tested. The stiffness, vertical yield capacity [15], and ultimate bearing capacity of the building-model containers are verified in [16], [17], which utilized the finite element analysis method to validate the maximum bearing capability of the container. However, previously designed schemes have mainly been verified for their feasibility and practicability in practical engineering construction, the security and reliability of the multi-modular container under the extreme weather events have not been studied yet.

Based on the advantages of container building [18] and tracked vehicle [19], a movable and self-extensible apparatus was developed and implemented in this paper to enhance the automation level of substation construction and security of maintenance personnel. Considering the extreme weather events such as snowstorms, strong wind, and the integrated blizzard conditions, the overall framework and control system of the apparatus is designed based on the finite element method. The modal analysis and static analysis under self-extensible mode are implemented to verify stability and rigidity for the assembled apparatus frame. The security evaluation for the apparatus is formulated by calculating the maximum displacement and ultimate stress under the severe weather events. Finally, the on-site application in the 500 kV substation of Hunan province validates the stability, practicability, and low-cost performance of the developed apparatus.

II. FRAMEWORK DESIGN OF THE APPARATUS

The designed apparatus frameworks in the normality and extension mode are depicted in Figure 1. The apparatus is 5 m long, 2 m wide and 2.5 m high. Joist steel and square steel are welded to form the framework. Stainless steel is used as the outer skin which is filled with the polyurethane foam for thermal insulation. The boards are connected by riveting, welding, or hinging. To realize the functions of the automatic elevator, translation, and rotation, the servo-drive system composed of servo motor, electric cylinder, and AX5000 servo driver is used to drive the apparatus. When the apparatus is extended, it can form an open workspace and a close rest area. The workspace is equipped with a complete set of pneumatic and electric tools to achieve the integration of standardized electrical components and the rest area is fixed with three air-conditioners and folding desks.

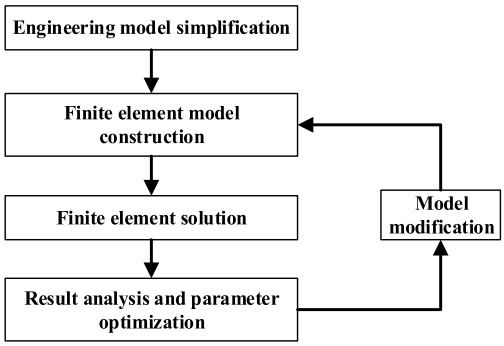

FIGURE 2. Flow chart of optimal design for main framework model.

III. DESIGN OF MAIN MODULES

A. EXTENSIBLE MAIN FRAMEWORK MODEL

In this paper, the main framework mainly comprised of the beam bottom, beam interval, and upright column is designed. Considering the stability and reliability, the simplified design concept is proposed to ensure the flexibility of the apparatus. The designed flow of the main framework model is shown in Figure 2.

The main framework of the apparatus uses Q235 steel which yield strength is 235MPa. The support foundation of the apparatus is made of 14# I-beam, while the main framework utilizes 80 × 80 square steel. The static load P is formulated as,

$$P = \frac{4fW_x}{L} \tag{1}$$

where f denotes the tensile strength of Q235, W_x is the sectional resistance moment, and L is the beam length.

The beam bottom utilizes six-interval plates of steel connected by high-strength hinges. The beam interval is optimally designed to meet folding and stretched requirements. In addition, as the key component of the main framework, the upright column adopts an H-beam structure and the expanding column adopts an angle-steel structure for conveniently installing the motor and drive components.

B. OUTER SKIN STRUCTURE DESIGN

Taking advantage of the light-steel structure, the outer skin is critical to the horizontal resistance of the entire apparatus. Its structure is not bolted connection but welded between the side plate and the frame. As the outer skin is selected as the standard part in the designing procedure, it is only replaced by a corrugated side plate. Figure 3 shows the calculation model of the side plate under uniform load.

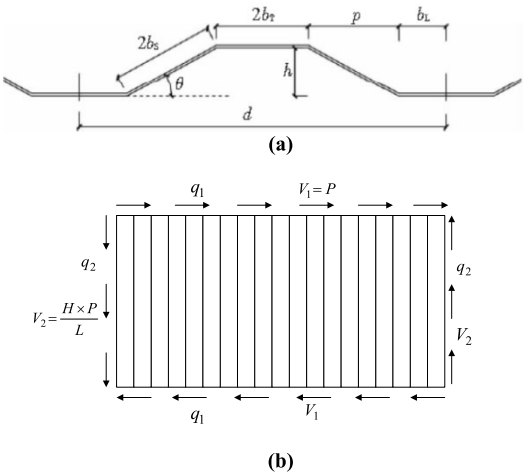

FIGURE 3. Calculation model of the side plate of outer skin structure: (a) a corrugation unit of the sidewall, (b) calculation model of sidewall under uniform load.

Assuming that the horizontal force of the upper beam is uniform, the calculated model is regarded as the cantilever beam model due to its small cross ratio. Ignoring the bending deformation, the side plate is subjected to shear force V_1 and V_2 (see Figure 3(b)). The shear strain γ of the side plate includes the pure shear strain γ_j and shear strain γ_n in the case of corrugation and distortion, which can be derived as,

$$\gamma_j = \left(1 + \frac{h}{d}\right) \times \frac{2(1+\nu)}{ELt} \times P \tag{2}$$

$$\gamma_n = \left(\frac{288 b_T \eta}{d}\right) \times \frac{\left(1-\nu^2\right) P}{E t^3 H^2 L} \tag{3}$$

Combining (2) and (3), the side plate stiffness K_b can be expressed as,

$$K_b = \frac{2P}{\left(\gamma_j + \gamma_n\right) \times H} \tag{4}$$

where h is the height of the side plate, d is the length of horizontal projection, v is Poisson's ratio, E is the elasticity modulus of Q235, t is the thickness of the side plate, η is a constant related to the corrugated shape of the side plate, and L is the sidewall length of the outer skin.

C. SPATIAL SELF-EXTENSIBLE MODEL

Combining the spatial expansion requirements, a spatial self-extensible structure with the electric cylinder and multi-bar folding is designed. Compared with the conventional drive mode using the hydraulic cylinder, the drive mode by the electric cylinder can avoid the drawbacks of hydraulic leakage and overweight. The self-extensible model is connected by three rods sets through the middle hinge pins. The upper and lower rods on both sides are fixed on the unfolding-terminal column and the main body column by hinges. The intermediate rods move vertically in their vertical directions with different self-extensible positions. The driving servo-motor and electric cylinder are connected to the intermediate rod at both sides. The expansion and recovery action of the folding rod module is driven by the telescopic movement of the electric cylinder, to realize the outward expansion and main body skeleton recovery of the apparatus. Figure 4 shows the schematic diagram of the folding rod module.

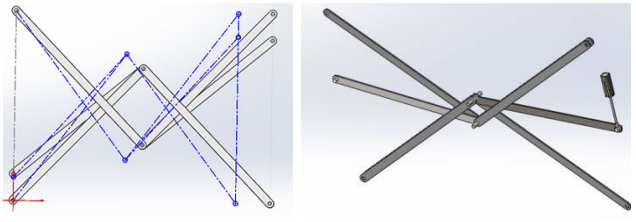

FIGURE 4. Schematic diagram of folding rod module.

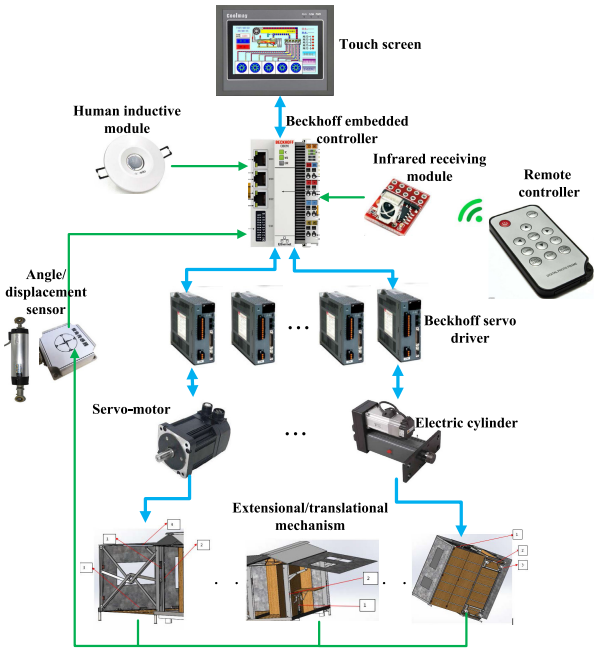

FIGURE 5. Control system framework of the apparatus.

D. CONTROL SYSTEM DESIGN

The control system of this apparatus mainly consists of touch screen, Beckhoff embedded controller (BEC), human inductive module, Beckhoff servo driver (BSD), servo motor or electric cylinder, and so on, as shown in Figure 5.

The working principle of the control system is divided into the following several steps. Firstly, when BEC receives the lifting or extensional instruction sending by the touch screen, the BEC will send the pulse to all the BSD. Then the BSD converts the received pulse into the signal and sends it to each motor or electric cylinder which rotated the appropriate angle to drive conjointly with the extensional or translational mechanism acting. The human inductive module attached directly to BEC is in charge of real-time monitoring whether people or live animals are in the apparatus or not. The infrared receiving module is applied to remotely control the stretching/ translation movement of the apparatus. The Angle /displacement sensor is used to transmit the angle and the real-time motion track to the controller to adjust the

control variable and ensure the stable operation of the system. Compared with the conventional hydraulic driving mode, the electric driving mode has an excellent practical performance with low pollution and high efficiency.

IV. SAFETY ANALYSIS UNDER EXTREME SITUATION

When the apparatus is applied in the smart substation, it is often necessary to carry out the expansion and folding operation. Due to the effect of variable torque, it may cause overturning if the apparatus is controlled inappropriately during the process of expansion and folding. Besides, extreme weather events may affect the secure operation of the apparatus in practical engineering. Therefore, three aspects of modal analysis, static analysis, and safe analysis under the extreme weather events are taken into account for tacking with the ultimate state. The modal analysis is implemented to verify the stability of the apparatus by analyzing the various vibration modes while static analysis is implemented to verify the rigidity of the apparatus by simulating the bearing capability.

A. MODAL ANALYSIS UNDER SELF-EXPANSION MODE

The initial state of apparatus self-expansion is that the self-loading device descends to 500mm. Before the test procedure, the four undersides of the self-loading device were adjusted to the fixed constraints according to the parameters requirement. In the simulation test, the self-loading device rises to the highest state that can be reached. The modal frequency of the first four orders is calculated as 1.7906Hz, 2.6Hz, 2.8718Hz, 4.2394Hz, respectively based on the finite element method. The vibration modes of the corresponding modal orders are shown in Figure 6.

In Figure 6, it can be seen that the maximum displacement is about 9 mm located in the connection position between the horizontal structure and the main body frame. Combined with the seismic frequency (generally 30Hz∼40Hz), the simulation results indicate that the unbalanced frame of the apparatus is suitable for the recommended safe requirement. Besides, the modal data is not similar to the general seismic frequency as well as the resonance range.

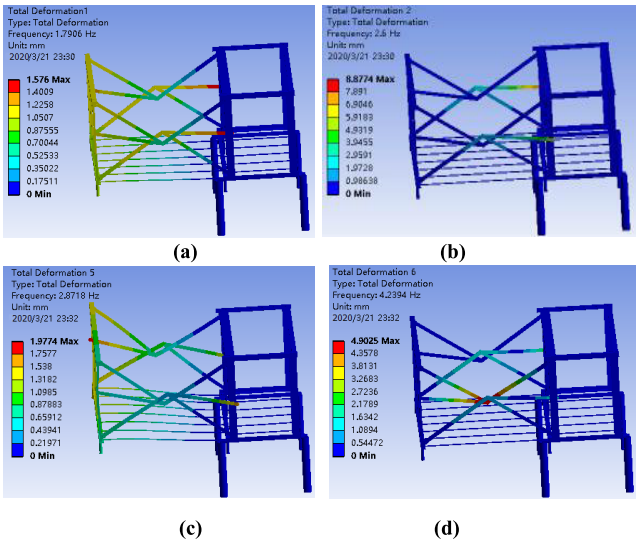

FIGURE 6. Modal analysis of the apparatus frame under the ultimate state: (a) f=1.7936Hz, (b) f=2.6Hz, (c) f=2.8718Hz, (d) f=4.2394Hz.

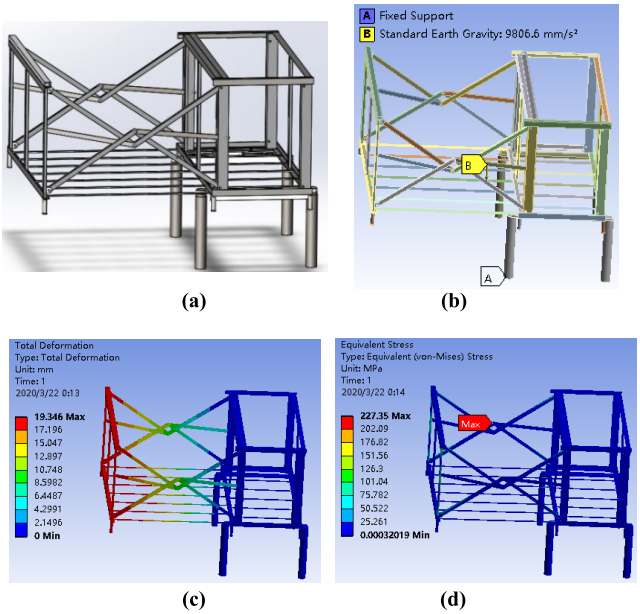

FIGURE 7. Static analysis of the apparatus frame under expansion mode: (a) static model, (b) static loading diagram, (c) displacement distribution, (d) ultimate strain distribution.

B. STATIC ANALYSIS UNDER SELF-EXTENSIBLE MODE

Considering the secure operation of the apparatus under expansion and folding mode, the initial state of the apparatus is that the self-loading device is lowered to 500mm. During the static simulation calculation process, the self-loading device is raised to the highest state that can be achieved, which aims to simulate and calculate the bearing capability of the apparatus under the self-gravity state.

Figure 7 depicts the static analysis results of the apparatus under self-extensible mode, the static loading was applied in the self-loading device. The test results verify that the apparatus frame can be able to stand the ultimate state. In particular, when the self-loading device rises to the highest state that can be reached, its gravity center will change due to the self-gravity effect. There is an approximate 20mm maximal displacement located in the pin roll spacing of adapting piece while the rest stress ignores. In addition, it can be found that the apparatus can safely fall and rise without overturning when it reaches the limit state of self-expansion mode.

C. SECURITY ANALYSIS UNDER EXTREME WEATHER EVENTS

When a movable self-extensible apparatus is applied in an actual substation, it is necessary to consider the rainstorm, snowstorm, strong wind, or other extreme weather events. Due to rainwater's liquidity, its transient load is less than a load of snow and wind imposed by the finite element analysis. Therefore, the extreme weather events in this paper mainly consist of the snowstorm, strong wind, and the integrated blizzard condition combining the above two. Figure 8 shows

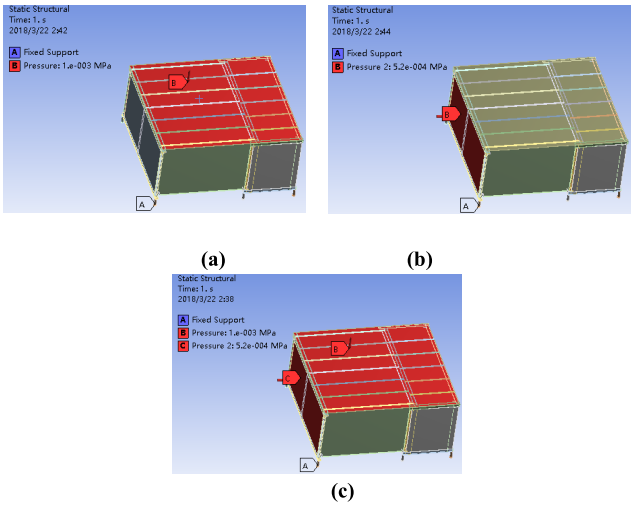

FIGURE 8. Loading simulation model: (a) snowstorm loading, (b) strong wind loading, (c) integrated blizzard.

the loading simulation model. By using ANSYS software, the calculation model based on the finite element method is established to analyze the maximum displacement and ultimate stress of the apparatus considering the extreme weather events.

According to the loading code for the design of building structures GB5009-2001, the standard value S_kS_k of snow load on the roof under snowstorm condition can be calculated as,

$$S_k = \mu_r S_0 \tag{5}$$

where μ_r is the snow distribution coefficient, S_0 is the basic snow pressure.

The standard value W_k of wind load under strong wind condition which is perpendicular to the roof is given by,

$$W_k = \beta_Z \mu_S \mu_Z W_0 \tag{6}$$

where β_Z is the vibration coefficient at height Z, μ_S and μ_Z are the shape coefficient and wind pressure height coefficient, respectively. W_0 is the basic wind pressure.

The conversion relation between wind speed and wind pressure W_0 is expressed as,

$$W_0 = \frac{\gamma}{2g} v^2 \tag{7}$$

Under the extreme weather events, we respectively adopt the gravity stack way and the hole-punching way to simulate the snow load and wind load. In particular, the counterweight is directly loaded in apparatus plates, the snow load is allotted equivalent to each load point according to the equivalence principle of mechanics. Meanwhile, the distributive girder of the jack is directly loaded in the windward side and roof of the apparatus. The integrated blizzard condition combines the snowstorm event with strong wind event. Under this severe circumstance, the loading model is built to verify the maximum bearing capability of the apparatus.

TABLE 1. Apparatus parameters.

Parameters	Symbol	Value
Tensile strength of I-beam Q235	f	$210\text{N}/mm^2$
Sectional resistance moment	W_x	$101.7cm^3$
Length of each beam	L	$5000mm$
Snow distribution coefficient	μ_r	2
Vibration coefficient	β_Z	1.0
Shape coefficient	μ_S	-0.5
Wind pressure height coefficient.	μ_Z	1.0

TABLE 2. Wind pressure of different parts under various wind speed levels.

Wind Pressure	Wind speed level		
	9	10	11
Wind speed (m/s)	23.5	28.4	32.3
Basic wind pressure (kN/m^2)	0.35	0.5	0.65
Roof of wind pressure (kN/m^2)	-0.175	-0.25	-0.325
Leeward wind pressure (kN/m^2)	-0.175	-0.25	-0.325
Wind pressure against windward (kN/m^2)	0.28	0.4	0.52

V. SIMULATION EVALUATION AND ON-SITE APPLICATION

In order to evaluate the reliability and practicability of the developed apparatus, a finite element simulation model By using ANSYS is established considering the ultimate loading tests. The apparatus parameters and wind pressure of different parts of the apparatus under different wind speed levels are illustrated in Tables 1 and 2, respectively.

A. FINITE ELEMENT MODEL AND ANALYSIS OF THE MAIN FRAMEWORK

The static analysis of the beam bottom is implemented to optimize the design of the main cased model. When applied the 20kN loads into the beam bottom, the finite element analysis results are shown in Figure 9. It can be seen that the elastic deformation appears in the middle of the beam bottom, and the deformation displacement is about 10 mm. The maximum stress is lower than 100N at the end of the beam bottom due to the smaller chamfer. Based on the above analysis, the tactful and obtuse design should be adopted to avoid the local stressed structure.

Analysis results of finite element strength for interval bottom, as shown in Figure 10, are calculated when loading the equivalent load of the pressure 0.02 MPa on the artifacts. The maximal displacement deformation (see Figure 10 (a)) is about 18mm, which appears in the middle of two-interval beams. The maximal stress is about 147 MPa, which is within the range of corresponding elastic deformation of steel components and meets the design requirements. In the designed procedure, the length of the bearing direction is adjusted to an appropriate value to enhance the stiffness of the beam and ensure the rigidity of the interval beam.

The finite element analysis of the comprehensive strength by taking the transverse offset and vertical directions into account is presented in Figure 11. The load test is performed as applying the 40kN loads on the top, while the lateral deflection load is 10000N. The maximum elastic deformation displacement is about 11.7mm, and the corresponding ultimate stress appears near the bottom of the reserved motor hole. The

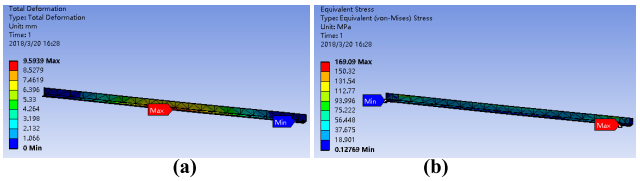

(a) (b)

FIGURE 9. Finite element analysis of beam bottom: (a) displacement distribution, (b) strain distribution.

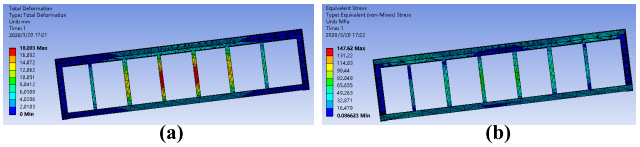

(a) (b)

FIGURE 10. Finite element analysis of interval bottom: (a) displacement distribution, (b) strain distribution.

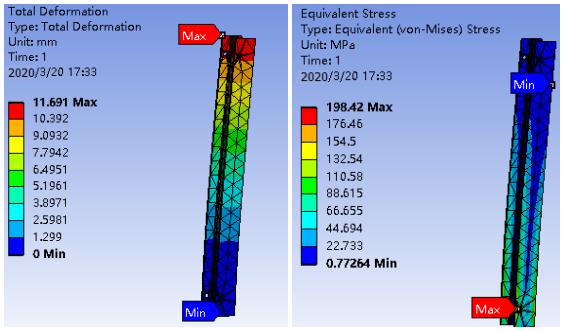

FIGURE 11. Finite element analysis of upright column (a) displacement distribution, (b) strain distribution.

test results indicate that the current upright column designed component is appropriate for the apparatus application.

B. SIMULATION RESULTS UNDER EXTREME WEATHER EVENTS

Under the extreme weather events, the gravity stack way and the hole-punching way is adopted to simulate the snow load and wind load. In particular, the counterweight is directly loaded in apparatus plates, the snow load is allotted equivalent to each load point according to the equivalence principle of mechanics. The wind speed level 11 is adopted in this case to model the strong wind condition. Meanwhile, the distributive girder of the jack is directly loaded in the windward side and roof of the apparatus.

The security evaluation results of the apparatus under various weather events are illustrated in Table3. It can be seen that the maximum displacement and the ultimate stress are less than the critical value [20]. These results not only demonstrate that the apparatus meets the operation demand under corresponding weather conditions, they likewise validate the stability and reliability of the integral structure of the apparatus.

C. ON-SITE APPLICATION AND COST ANALYSIS

The designed apparatus has implemented in 10 substations of China, such as 500 kV Minfeng substation in Loudi city, 220 kV Jiuhua substation in Xiangtan city, and 110 kV Guangsheng substation in Changsha city. Figure 12 shows the on-site application of the apparatus in the Minfeng substation.

TABLE 3. Simulation results under various weather events.

Weather Events	Maximum Displacement (mm)	Ultimate Stress (MPa)
Snowstorm	11.14	148.65
Strong wind	10.97	105.9
Integrated blizzard	10.934	140
Critical value	27.78	235

(a) (b)

FIGURE 12. On-site application of the apparatus in the substation: (a) normality mode, (b) extension mode.

TABLE 4. Cost comparison results of the two devices.

Device	Construction Cost ($)	Operation Cost ($)
Developed apparatus	36450	1450
Fixed maintenance apparatus	437360	3000

The substation with 2×750 MVA transformers and 40 circuit breakers covers an area of 65000 square meters, which takes approximately two months every year for electrical infrastructure maintenance. The actual application demonstrates the maintenance time has decreased to 25 days by using the apparatus. Besides, the apparatus can admirably enhance working efficiency with characteristics of low cost, automatic control, excellent insulation, easy operation as well as high reliability.

Table 4 lists the comparative results of the designed apparatus and fixed maintenance apparatus on construction cost and operation cost in this substation. The designed apparatus can reduce about 90% construction cost and more than 50% operation cost compared with the fixed maintenance infrastructure.

VI. CONCLUSIONS

In this paper, a movable and self-extensible apparatus is designed, which can greatly improve working efficiency and reduce costs in the substation construction and electrical infrastructure maintenance. The simulation results indicate that the designed apparatus greatly meets the security and reliability in substation under the severe environment condition. The on-site application in the 500 kV substation of Hunan province validates the stability and practicability of the developed apparatus under various extreme weather events.

REFERENCES

[1] *Technical guide for smart substation*, (in Chinese), State Grid Cooperation of China, Beijing, China 2009.

[2] Q. Huang, S. Jing, J. Li, and D. Cai, "Smart substation: State of the art and future development," *IEEE Trans. Power Del.*, vol. 32, no. 2, pp. 1098–1106, Dec. 2017.
[3] S. Jing, Q. Huang, J. Wu, and W. Zhen, "A novel whole-view test approach for onsite commissioning in smart substation," *IEEE Trans. Power Del.*, vol. 28, no. 3, pp. 1715–1722, Jul. 2013.
[4] S. R. Etesami, W. Saad, N. B. Mandayam, and H. V. Poor, "Stochastic games for the smart grid energy management with prospect prosumers," *IEEE Trans. Autom. Control*, vol. 63, no. 8, pp. 2327–2342, Aug. 2018.
[5] D. Xu, Q. Wu, B. Zhou, C. Li, L. Bai, and S. Huang, "Distributed multi-energy operation of coupled electricity, heating and natural gas networks," *IEEE Trans. Sustain. Energy*, early access, Dec. 23, 2020, doi: 10.1109/TSTE.2019.2961432.
[6] H. Wang, Y. Liu, B. Zhou, C. Li, G. Cao, N. Voropai, and E. Barakhtenko, "Taxonomy research of artificial intelligence for deterministic solar power forecasting," *Energy Convers. Manage.*, vol. 214, Jun. 2020, Art. no. 112909.
[7] H. Wang, D. Lin, J. Qiu, L. Ao, Z. Du, and B. He, "Research on multiobjective group decision-making in condition-based maintenance for transmission and transformation equipment based on D-S evidence theory," *IEEE Trans. Smart Grid*, vol. 6, no. 2, pp. 1035–1045, Mar. 2015.
[8] Q. Wang, Z. He, S. Lin, and Y. Liu, "Availability and maintenance modeling for GIS equipment served in high-speed railway under incomplete maintenance," *IEEE Trans. Power Del.*, vol. 33, no. 5, pp. 2143–2151, Oct. 2018.
[9] H. Slawik, J. Bergmann, and M. Buchmeier, "Container atlas: A practical guide to container architecture," *Gestalen Verlag*, vol. 11, no. 6, pp. 66–70, 2010.
[10] J. Kotnik, "New container architecture: Design and sustainability," *Links Int.*, vol. 25, no. 3, pp. 61–67, 2013.
[11] Y. Zuo and X. Zha, "FEM and experimental study on mechanical property of integrated container building," *Int. J. Steel Struct.*, vol. 18, no. 2, pp. 699–718, Jun. 2018.
[12] H. Islam, G. Zhang, S. Setunge, and M. A. Bhuiyan, "Life cycle assessment of shipping container home: A sustainable construction," *Energy Buildings*, vol. 128, pp. 673–685, Sep. 2016.
[13] T. Bárvik, A. G. Hanssen, S. Dey, H. Langberg, and M. Langseth, "On the ballistic and blast load response of a 20 ft ISO container protected with aluminium panels filled with a local mass—Phase I: Design of protective system," *Eng. Struct.*, vol. 30, no. 6, pp. 1605–1620, Jun. 2008.
[14] K. Giriunas, H. Sezen, and R. B. Dupaix, "Evaluation, modeling, and analysis of shipping container building structures," *Eng. Struct.*, vol. 43, pp. 48–57, Oct. 2012.
[15] Y. Li, H. Wang, H. Qian, Y. Lei, and Q. Bai, "Effect of autoclaved lightweight concrete panels on the mechanical performance of container building and its equivalent method," *Adv. Struct. Eng.*, vol. 21, no. 7, pp. 1103–1116, May 2018.
[16] Y. Li, R. Ma, and Y. Li, "Numerical analysis on longitudinal stiffness and ultimate strength of single container for modular freight container buildings," *Pro. Steel Building Struct.*, vol. 16, pp. 28–33, 2014.
[17] S. Liu, M. Zheng, and B. Li, "Finite element analysis of the transverse rigidity of module container building," *J. Liaoning Univ. Technol.*, vol. 38, pp. 33–37, 2018.
[18] P. Jeyapandiarajan, G. Kalaiarassan, J. Joel, R. Shirbhate, F. F. Telare, and A. Bhagat, "Design and analysis of chassis for an electric motorcycle," *Mater. Today, Proc.*, vol. 5, no. 5, pp. 13563–13573, 2018.
[19] X. Han, H. He, J. Wu, J. Peng, and Y. Li, "Energy management based on reinforcement learning with double deep Q-learning for a hybrid electric tracked vehicle," *Appl. Energy*, vol. 254, Nov. 2019, Art. no. 113708.
[20] *Technical Code for Steel Structure of Light-Weight Building With Gabled Frames*, Standard 51022, 2015.

JUAN WEI received the B.S. and M.S. degrees in electrical engineering from North China Electric Power University, Beijing, China, in 2011 and 2014, respectively. She is currently pursuing the Ph.D. degree with the College of Electrical and Information Engineering, Hunan University, Changsha, China. She was a Visiting Student with the Department of Electrical Engineering, Technical University of Denmark, Kongens Lyngby, Denmark, from 2019 to 2020. Her research interests include wind power modeling and control, renewable energy generation, and power system secure operation.

DIANSHENG LUO (Member, IEEE) was born in Hunan, China, in 1971. He received the B.S., M.S., and Ph.D. degrees in power engineering from Jilin University, Changchun, China, in 1994, 1997, and 2000, respectively. He joined Hunan University, in 2001, where he is currently a Professor with the College of Electric and Information Engineering. He has authored or coauthored more than 110 journal articles and conference papers. His research interests include outdoor insulation online detection of power equipment, image processing, load forecasting, smart grid, renewable energy, power quality, demand side management, and smart home.

BOZHONG WANG received the B.S. and M.S. degrees in electrical engineering from North China Electric Power University, Beijing, China, in 2009 and 2012, respectively. He is currently a Power Grid Engineer with State Grid Hunan Electric Power Corporation Maintenance Company, Changsha, China. His major research interests include power system operation, reliability, and maintenance.

HONGYING HE (Member, IEEE) received the B.S. degree in electronic engineering from Jilin University, Changchun, China, in 1998, and the Ph.D. degree in electrical engineering from Hunan University, Changsha, China, in 2006. She is a member of IAS. She joined Hunan University in 2007, where she is an Associate Professor with the College of Electric and Information Engineering. Her fields of interests mainly include high voltage insulation detection, electric power equipment fault identification, load forecasting, image processing, and artificial intelligence. She was a recipient of the Best Symposium Paper Award at the IEEE International Meeting of Industry Applications Society, in 2018.

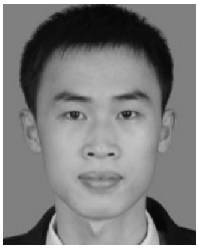

JINMING LI received the B.S. and M.S. degrees in electrical engineering from the South China University of Technology, Guangzhou, China, in 2011 and 2014, respectively. He is currently a Power Grid Engineer with the State Grid Hunan Economy Institute, Changsha, China. His major research interests include power system planning and reliability.

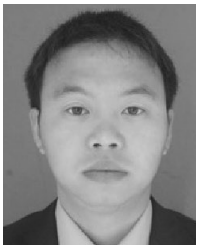

YULIN LUO received the B.S. degree in electrical engineering from the Changsha University of Science and Technology, Changsha, China, in 2011. He is currently a Power Grid Engineer with State Grid Hunan Electric Power Corporation Maintenance Company, Changsha. His major research interests include power system secure operation and maintenance.